Density functional simulations of Te-based phase change materials

J. Akola [1,2] and R. O. Jones [1]
[1] Institut fur Festkörperforschung, Forschungszentrum Jülich, D-52425 Jülich, Germany
[2] Nanoscience Center, Department of Physics, P.O. Box 35, FI-40014 University of Jyväskylä, Finland
jaakko.akola@phys.jyu.fi r.jones@fz-juelich.de

ABSTRACT

The structures of the amorphous, liquid, and crystalline phases of phase-change materials (PCM) and the rapid changes between them have motivated density functional (DF) simulations of Te-based materials on IBM Blue Gene supercomputers. We have simulated GeTe (50:50), $Ge_{15}Te_{85}$ (15:85), $Ge_2Sb_2Te_5$ (GST, DVD-RAM), and Te using large samples (216-630 atoms) over hundreds of picoseconds. If atoms are classified as type A (Ge,Sb) or B (Te), we observe pronounced AB alternation, and the main structural motif is a four-membered ABAB ring ("ABAB square"). The amorphous-to-crystalline transition may be viewed as a reorientation of disordered ABAB squares, since the metastable NaCl structure corresponds to perfect ordering. The coordination numbers of these systems (including Te) deviate from the "8-*N* rule", where *N* is the number of valence electrons: Te atoms have near threefold coordination and show a marked medium- to long-range order in GST. Octahedral bond angles predominate. The bond and dihedral angles of Ge atoms (predominantly fourfold coordinated) show tetrahedral and (distorted) octahedral local environments that change with Ge concentration. The disordered alloys contain cavities ("voids") that are analogous to the vacancies in crystalline compounds. We compare GeTe, $Ge_{15}Te_{85}$, and $Ge_2Sb_2Te_5$ and show the importance of homopolar ("wrong") bonds and vacancies (cavities). Some limitations of the theoretical methods are discussed.

Key words: Phase change materials, density functional calculations, molecular dynamics, $Ge_2Sb_2Te_5$ (GST), GeTe, $Ge_{15}Te_{85}$.

1. INTRODUCTION

The close relationship between the properties of a material and its atomic arrangement ("structure") is important in many areas of physics, chemistry, and biology. It is certainly true in materials science. Knowledge of the structures of the phases involved is essential to develop our understanding of the properties of *phase-change materials*, and theory has a decisive role to play. In principle, one needs "only" to calculate the total energy of an aggregate of atoms for different atomic arrangements and temperatures and locate low-energy structures, but the practical problems of doing so are immense. Density functional calculations involve no adjustable parameters, and the combination with molecular dynamics (the Car-Parrinello method [1]) has had a dramatic effect in materials science and chemistry. The demands on computational resources are very large, however, and the vast majority of simulations have been limited to systems with less than 100 atoms over some tens of picoseconds. These are profound restrictions for multi-element materials (which may also include cavities) where the time scale of the phase changes is longer than a nanosecond. A common alternative, particularly in biological systems, is to parameterize the energy in terms of a classical force field. This allows us to calculate thousands of atoms over physically relevant time scales, but it requires the development of a force field with predictive value in systems with several atom types. This is extremely difficult in practice, and our first calculations on phase change materials were carried out in support of such a project.

Density functional calculations allow us to develop an extensive (and extendible) database of structural information that can be used for determining or refining the parameters of a classical force field. The structures, relative energies, and vibration frequencies of clusters of selenium made possible the development of a force field for this element [2], and similar studies on sulphur [3] and phosphorus [4] were carried out in our group. Classical force fields were developed that reproduced some experimental information as well as DF results on small clusters of the elements. Monte Carlo calculations on over 2000 sulphur atoms provided new insight into ring-opening polymerization of liquid

sulphur, and calculations on 4000 phosphorus atoms providing much information about phase changes in the liquid under high pressure. When two colleagues (H. R. Schober, K. Schroeder) expressed interest in doing the same for GeTe, we carried out DF calculations on Te clusters as well as short MD/DF simulations on GeTe to provide a similar data base. However, it proved to be impossible to find parameters that could describe the melting temperature of Ge itself, much less the combination with another element. This occurred just before the first IBM BlueGene supercomputer was installed in the FZ Jülich, which prompted us to carry out combined MD/DF calculations on GeTe and related materials on a scale not previously possible. We describe here some of our work related to GeTe (50:50), $Ge_{15}Te_{85}$ (15:85), and $Ge_2Sb_2Te_5$ [5-7]. More details are provided in the original papers.

2. METHOD OF CALCULATION

The density functional calculations were performed with the Car-Parrinello molecular dynamics package CPMD [8] with the generalized gradient approximation of Perdew, Burke and Ernzerhof (PBE) [9] for the exchange-correlation energy functional. The electron-ion interaction was described by ionic pseudopotentials with the form of Troullier and Martins [10]. The program employs periodic boundary conditions, usually with one point (**k**=0) in the Brillouin zone, and the kinetic energy cutoff of the plane wave basis was 20 Ry. GST is modeled at the densities of the metastable crystalline (0.0331 atoms/Å^3) and amorphous (0.0308 atoms/Å^3) phases. The simulations were based on the rock salt lattice (crystalline GST) with 512 atomic sites, where the Na and Cl sites are occupied by Ge/Sb atoms (20 % each) and vacancies (10 %), and Te atoms (50 %), respectively. The Na sites are populated randomly with Ge, Sb, and vacancies, so that the system contains 460 atoms (102 Ge, 102 Sb, 256 Te) and 52 vacancies. The sizes of the cubic simulation boxes for the crystalline and amorphous phases are 24.05 Å and 24.62 Å, respectively. The GeTe system contains 216 atoms at the density of the amorphous phase (0.0335 atoms/Å^3), and the box size is 18.61 Å. The corresponding values for $Ge_{15}Te_{85}$ are 0.02827 atoms/Å^3 and 19.70 Å.

The use of Born-Oppenheimer MD, where the orbital eigenfunctions are optimized for each ionic configuration, has been decisive in the present work. The atomic numbers of Ge, Sb, and Te (32, 51, 52) are relatively large, and an efficient predictor-corrector method is used to converge the eigenfunctions. The time steps [250 and 125 a.u. (6.050 and 3.025 fs) for initialization and data collection, respectively] are much longer than in the usual Car-Parrinello approach, and the approach has crucial advantages in the metallic systems that arise at high temperatures in all alloys discussed here. Memory of the crystalline starting structure [Figure 1(a)] was erased by starting the simulations at 3000 K (liquid), followed by gradual cooling over 42 ps to the melting point (900 K). The first data collection was performed for 21 ps at 900 K, followed by cooling to 300 K over 139 ps. The second data collection (at 300 K) was also performed for 21 ps. Finally, the system was quenched to 100 K over 74 ps, and the resulting structure optimized using Car-Parrinello MD and simulated annealing [Figure 1(b)]. A similar cooling procedure for GeTe took a total of 340 ps, including data collection at 1000 K (45 ps) and 300 K (26 ps). In the case of $Ge_{15}Te_{85}$, data were obtained at 680 K (liquid, 47 ps) and 300 K (amorphous, 31 ps) in a total simulation time of 300 ps.

MD methods allow us to follow the coordinates R_i and velocities v_i of all atoms throughout the simulations. This leads directly to pair correlation functions g_{ij} for pairs of atom types and, via an appropriate Fourier transformation, to the structure factor $S(Q)$. Insight into the local order can be found from the distributions of the bond and dihedral angles and by defining local order parameters similar to those used in the theory of binary liquids [5]. In discussing order, it is convenient to separate atoms into types A (Ge, Sb) and B (Te). The vibration frequencies at a given temperature can be determined from (a) simulation trajectories by Fourier trans-forming the velocity-velocity auto-correlation function or (b) by

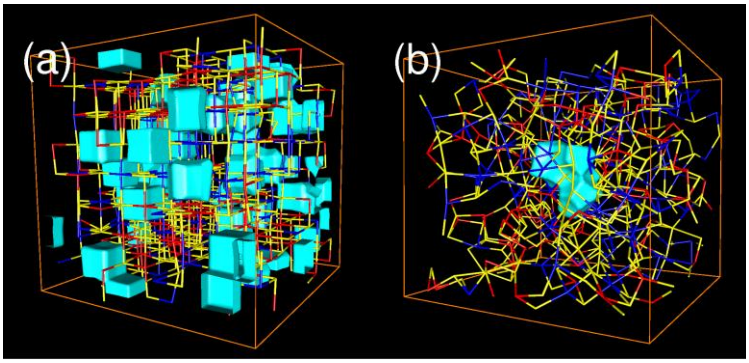

Figure 1. Simulation of GST with 460 atoms and 52 vacancies in (a) c-GST and (b) a-GST. Red: Ge, blue: Sb, yellow: Te. Vacancies (cavities) are shown as light blue surfaces. A single large cavity (multivacancy) is shown in (b).

diagonalizing the dynamical matrix calculated for a well-equilibrated sample.

3. RESULTS AND DISCUSSION

A. $Ge_2Sb_2Te_5$ (GST)

The most striking feature of the partial radial distribution functions (Figure 2) is the medium- to long-range order found among Te atoms up to 10 Å, with peaks at 4.16 Å and 6.14 Å, a minimum at 5.4 Å, and additional maxima at 7.8 Å and 9.8 Å. The weak maximum at 2.95 Å and the low coordination number (0.3) show that there are few Te-Te bonds. There is no significant order at 900 K. Te atoms prefer coordination with Ge/Sb, with Te forming the second-neighbour shell. Thermal fluctuations in c-GST lead to peak broadening. The "homopolar" Ge-Ge, Ge-Sb, and Sb-Sb bonds in the three phases are shown in Figure 2. While these bonds are absent in c-GST, they occur in the amorphous phase ("wrong bonds"). They have small weight, and the average coordination numbers are between 0.2 and 0.6. Heating to 900 K results in significant changes in the Ge-Ge and Ge-Sb curves: the first peak now dominates, and the order between 4 and 7 Å moves to shorter range.

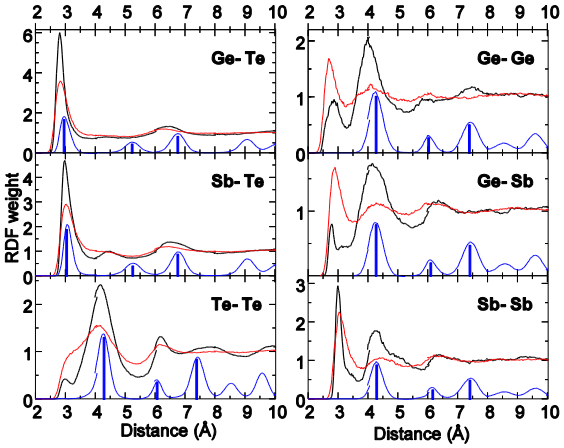

Figure 2. Partial RDF of a- (thick black) and l-GST (red/grey). Blue curve and bars (different scale) are for c-GST at 300 K.

All coordination numbers for a-GST (Ge: 4.2, Sb: 3.7, Te: 2.9) are lower than in the crystal, but larger than the values (4, 3, 2) suggested by the "8-*N*" rule, where *N* is the number of valence electrons. The coordination numbers show that l-GST (900 K) is less ordered than the amorphous state. Bond angle distributions around Ge and Sb (not shown) show octahedral features (a pronounced maximum at 90°and a weaker peak at 180°), and Sb is more strongly peaked than Ge. Radial and angular distribution functions as well as coordination numbers show interesting differences as the temperature changes. For details, see [5] and [6].

The similarities between ring statistics in amorphous and crystalline GST have been proposed as the basis for the structural phase change in GST [11]. The statistics of all irreducible loops (rings) in a- and l-GST have been calculated using a bond cutoff of 3.2 Å and periodic boundary conditions (Figure 3). Fourfold rings dominate the statistics at 300 K, and the contribution of ABAB rings (squares) is 86 % of the total. 52 % of atoms participate in at least one ABAB configuration. An example of a structure with ABAB alternation is given in Figure 4, where we also show that an alternating *cubic* structure can occur.

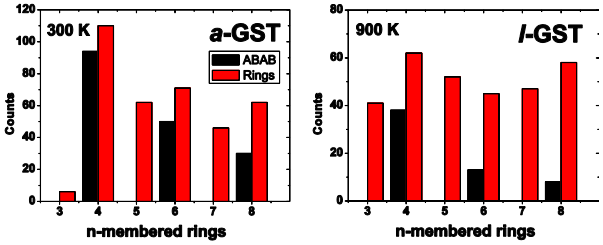

Figure 3. Ring statistics for a-GST (300 K) and l-GST (900 K). ABAB: even-membered rings with bond alternation.

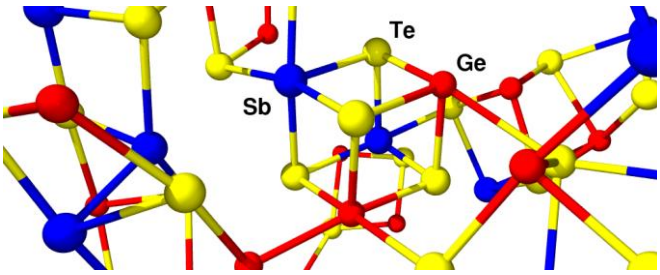

Figure 4. A cubic ABAB unit in a-GST. A Ge-Ge bond and a Sb-Sb bond are evident.

Cavities play an essential role in Ge/Sb/Te alloys. Since crystalline GST contains 10% vacancies, a-GST, whose density is 7% lower, must contain empty regions (cavities or voids, see Figure 1). We have developed [5] a method for assigning cavities and determining their volumes, and we estimate that they comprise 11.8 % of the total volume of a-GST (slightly more than in the crystal), and this increases to 13.8 % at 900 K.

The electronic density of states (DOS) and its projections are shown in Figure 5. The DOS curves have a three-peak structure characteristic of materials with average valence five: the two lowest bands can be assigned to s-electrons (σ-band), while the broad band between -5 eV and the Fermi energy has p-character (π-band). The calculations for c- and a-GST show band gaps of around 0.2 eV at the Fermi energy.

Photoemission measurements have shown that there are significant differences in the valence band DOS and the core levels of a- and c-GST and other Ge/Sb/Te alloys [12]. The differences measured by hard x-ray photoemission spectroscopy (XPS, [12]) are compared with our results in Figure 5. The agreement is remarkably good, particularly for the DOS difference [Figure 5(c)].

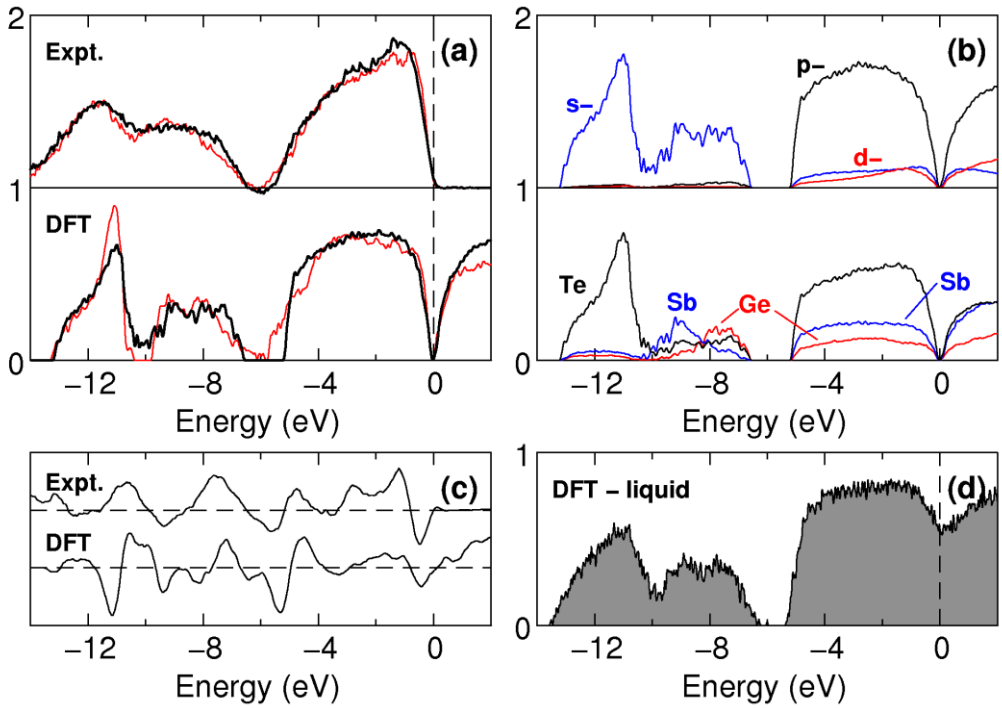

Figure 5. (a) XPS valence band spectrum of c- (thick black) and a-GST (red/grey) [Ref. 12, upper panel] and the calculated electronic DOS (lower panel). (b) Theoretical DOS projected onto atom-centred s-, p-, and d-components and atomic types. (c) DOS difference between c-GST and a-GST [from panel (a)], where positive values indicated a larger weight on a-GST. (d) Electronic DOS of liquid GST. The vertical dashed lines mark the Fermi energy.

The vibration frequencies provide important structural information about condensed matter and molecules, and we have calculated the frequency distributions in two ways: (a) from the Fourier transform of the velocity-velocity autocorrelation function, calculated from trajectories of 6000 time steps of 3.025 fs each, and (b) from the dynamical matrix calculated from the second-order energy derivatives of a well-equilibrated structure. The results for a-GST (Figure 6) show that the agreement between the results for the two methods is very good. The most pronounced features are peaks near 60 cm^{-1} and 150 cm^{-1} and a tail for frequencies above 180 cm^{-1}. Projections onto the vibrations

of different elements and structural units show that the tail is associated with the vibrations of the lightest element Ge, particularly atoms that are fourfold coordinated.

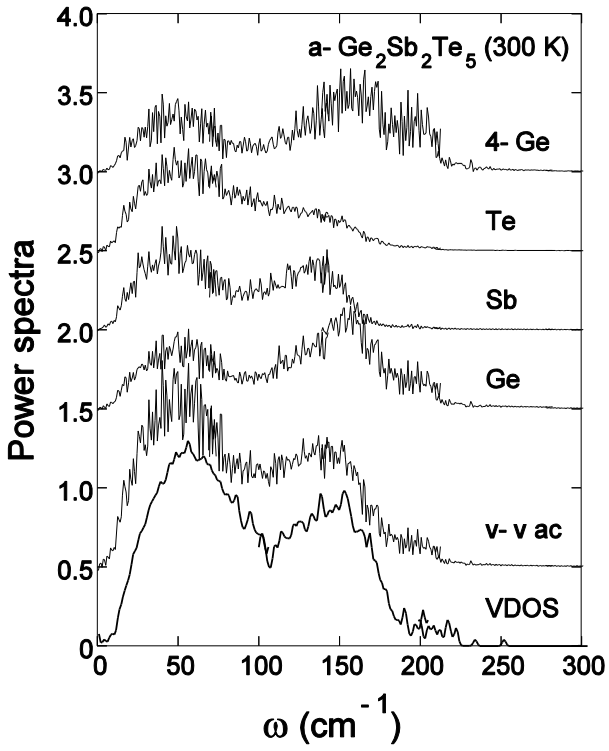

Figure 6. Calculated vibrational density of states for a well-equilibrated sample of a-GST (VDOS, lowest curve) and power spectra form simulation trajectories for a-GST, for Ge, Sb, and Te, and for fourfold coordinated Ge atoms (4-Ge).

B. GeTe and $Ge_{15}Te_{85}$

Binary alloys of Ge and Te have fascinated experimentalists and theorists for decades. They were among the first to show real promise as phase change media [13], and there are striking changes on melting, particularly near the eutectic composition $Ge_{15}Te_{85}$ (15:85). In [5] we presented the results of simulations of a-GeTe with 216 atoms in the unit cell and compared the results with those of a-GST. In both cases there is medium- to long-range order of Te atoms and the crucial structural motif is a four-membered ABAB ``square''. The amorphous to crystalline phase change can then be viewed as a reorientation of such units to form an ordered lattice. The deviations from the ``8-*N*'' rule that are found for GST apply also to GeTe.

We have performed simulations for the eutectic mixture $Ge_{15}Te_{85}$ [6] and compare the partial RDF with those of GeTe in Figure 7. There is no sign of medium- to long-range order in $Ge_{15}Te_{85}$. Amorphous GeTe has few Te-Te bonds, while Ge-Ge bonds are rare in $Ge_{15}Te_{85}$. The average coordination

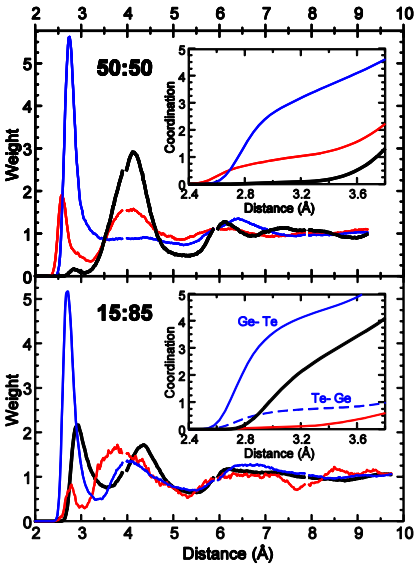

Figure 7. Partial RDF of a-GeTe and a-$Ge_{15}Te_{85}$ at 300K. Black (thick) line, Te-Te; blue (peaked) Ge-Te; red (middle), Ge-Ge. Insets: coordination numbers as a function of cutoff distance

numbers are 4 for Ge and 3 for Te, and the most prominent configurations in GeTe and $Ge_{15}Te_{85}$ are Ge-$GeTe_3$ and Ge-Te_4, respectively. Ge atoms can be tetrahedrally and octahedrally bonded, and the former dominate in 15:85. Atoms in GeTe favour octahedral or cubic bond angles, although sixfold coordination is found in only 3.4 % and 11.0 % of Ge atoms at 300 K and 1000 K, respectively. Corner and edge-sharing Ge-Te_4 tetrahedra are common in $Ge_{15}Te_{85}$. The threefold (cubic) coordination of Te in both GeTe and $Ge_{15}Te_{85}$ deviates from the predictions of the "8-*N*" rule.

As in GST, ABAB squares are essential for the phase transition in GeTe (Figure 8). In a-GeTe, 75 % of the atoms are involved. Even above the melting point (1000 K), 41 % of the atoms participate in ABAB squares. Cavities are characteristic of $Ge_{15}Te_{85}$, occupying more than 25 % of the total volume in both amorphous and liquid states [see Figure 8(b)]. The volumes and shapes very widely, and the cavity distributions depend significantly on the temperature. There are more cavities in the liquid (680 K) and more that are smaller, whereas larger cavities (70-100 $Å^3$) are more abundant at 300 K.

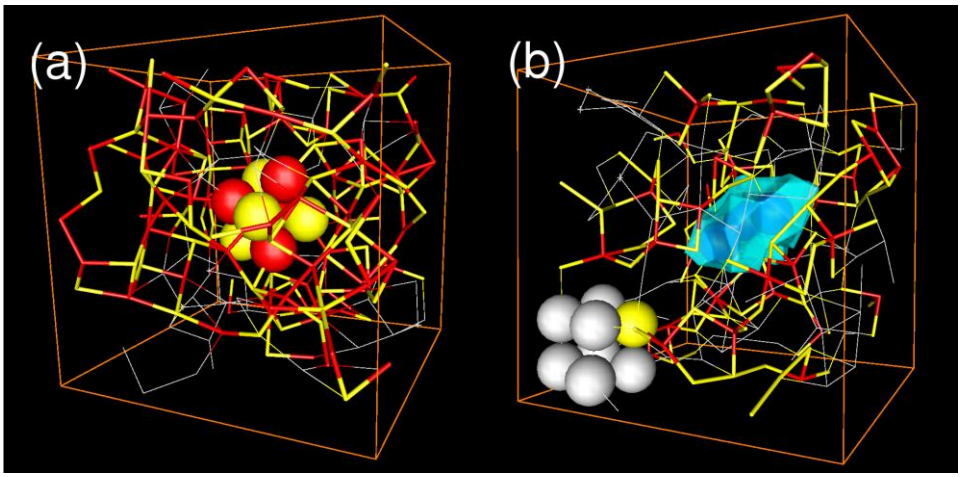

Figure 8. (a) Simulation box of a-GeTe (18.6 Å, 216 atoms) with ABAB squares highlighted. An ABAB cube is shown. Red: Ge, yellow: Te. (b) Simulation box of $Ge_{15}Te_{85}$ (19.7 Å, 216 atoms) with Ge and Ge-coordinating Te atoms highlighted. A multivacancy and a Te cube are also shown.

4. CONCLUDING REMARKS

We have summarized here results of our massively parallel simulations (IBM Blue Gene computers) on $Ge_2Sb_2Te_5$ (GST), GeTe, and $Ge_{15}Te_{85}$. The availability of computers of this class as well as efficient algorithms make density functional calculations possible for systems with hundreds of atoms over time scales of hundreds of picoseconds, i.e. approaching the crystallization time of phase change materials. This is an immensely encouraging development. The calculations have enabled us to identify the crucial pattern ("ABAB squares") in the phase transition in GST [14], and to study the differences between GeTe and both GST and $Ge_{15}Te_{85}$. This approach will certainly continue to provide insight into the behaviour of these and other materials of interest to the phase-change community.

Some words of caution are, however, appropriate. One of the most remarkable results of this study was the discovery of medium- to long-range order in Te atoms in amorphous GST and GeTe, and this would be impossible to detect in simulations of fewer atoms. This is also true for studies of cavities, which can occur as large multivacancies in these systems. It is also crucial that the liquid state be cooled over a time scale that is physically relevant. The use of Born-Oppenheimer MD with an efficient predictor-corrector scheme for converging the orbital eigenfunctions has been decisive. The time steps are two orders of magnitude greater than in many other systems, and this is aided by the high atomic numbers of the component elements. Furthermore, high temperatures favour metallic samples in these systems, and the absence of a gap in the eigenvalue spectrum often leads to instabilities in the Car-Parrinello approach. Similar

findings were found in another study of GST [15]. Such calculations are a major undertaking at the present time, both in terms of computational resources and the effort required to analyze the results, and this situation is unlikely to change in the short term.

Work continues on these and other projects. Of particular interest to researchers both within and outside the phase change community is elemental tellurium, for which experimental and calculated structure factors and pair distribution functions often disagree. We have found that the results of DF calculations of structural properties of Te depend significantly on the choice of the functional form used for the exchange-correlation energy. While it is encouraging that the best agreement with experiment is obtained using recently developed functionals that go beyond the gradient of the density (such as TPSS [16]), this observation means that it is appropriate to perform such checks in general.

The calculations were performed on IBM Blue Gene/L, Blue Gene/P, and p690 computers in the Forschungszentrum Jülich with grants from the FZ Jülich and the John von Neumann Institute for Computing. We thank S. Kohara, K. Kobayashi, and T. Matsunaga for helpful discussions and original data.

REFERENCES

1. R. Car and M. Parrinello, "Unified approach for molecular dynamics and density functional theory", Phys. Rev. Lett. **55** (1985) 2471

2. C. Oligschleger, R. O. Jones, S. M. Reimann, and H. R. Schober, "Model interatomic potential for simulations in selenium", Phys. Rev. B **53** (1996) 6165.

3. P. Ballone and R. O. Jones, "Density functional and Monte Carlo studies of sulfur", J. Chem. Phys. **119** (2003) 8704.

4. P. Ballone and R. O. Jones, "A reactive force field simulation of liquid-liquid phase transitions in phosphorus", J. Chem. Phys. **121** (2004) 8147.

5. J. Akola and R. O. Jones, "Structural phase transitions on the nanoscale: The crucial pattern in the phase-change materials $Ge_2Sb_2Te_5$ and GeTe'', Phys. Rev. B **76** (2007) 235201.

6. J. Akola and R. O. Jones, "Binary alloys of Ge and Te: Order, voids, and the eutectic composition", Phys. Rev. Lett. **100** (2008) 205502.

7. J. Akola and R. O. Jones, "Density functional study of amorphous, liquid and crystalline $Ge_2Sb_2Te_5$: Homopolar bonds and/or AB alternation", (submitted).

8. CPMD V3.11: copyright IBM Corporation 1990-2006; copyright MPI für Festkörperforschung, Stuttgart 1997-2001 (http://www.cpmd.org).

9. J. P. Perdew, K. Burke, and M. Ernzerhof, "Generalized gradient approximation made simple", Phys. Rev. Lett. **77** (1996) 3865.

10. N. Troullier and J. L. Martins, "Efficient pseudopotentials for plane-wave calculations", Phys. Rev. B **43** (1991) 1993.

11. S. Kohara et al.. "Structural basis for the fast phase change of $Ge_2Sb_2Te_5$: Ring statistics analogy between the crystalline and amorphous states", Appl. Phys. Lett. **89** (2006) 201910.

12. J-J. Kim et al. "Electronic structure of amorphous and crystalline $(GeTe)_{1-x}(Sb_2Te_3)_x$ investigated using hard x-ray photoemission spectroscopy", Phys. Rev. B **76** (2007) 115124.

13. M. Chen, K. A. Rubin, and R. W. Barton, “Compound materials for reversible phase-change optical data storage”, Appl. Phys. Lett. **49** (1986) 502.

14. Subsequent calculations support this assignment. See, for example, J. Hegedüs and S. R. Elliott, “Microscopic origin of the fast crystallization ability of Ge-Sb-Te phase-change memory materials”, Nature Mater. **7** (2008) 399.

15. S. Caravati, M. Bernasconi, T. D. Kühne, M. Krack, and M. Parrinello, “Coexistence of tetrahedral- and octahedral-like sites in amorphous phase change materials”, Appl. Phys. Lett. **91** (2007) 171906.

16. J. Tao, J. Perdew, V. N. Staroverov, and G. E. Scuseria, “Non-empirical meta-generalized gradient approximation designed for molecules and solids”, Phys. Rev. Lett. **91** (2003) 146401.

Biographies

J. Akola studied Physics at the Universities of Helsinki and Jyväskyla, Finland, obtaining his Ph.D. at Jyväskylä under Matti Manninen. After five years as a Post-doctoral Researcher at the Forschungszentrum Jülich, Germany, he returned in 2005 to the Nanoscience Center in Jyväskylä. His fields of interest include classical tight-binding and density functional simulations of materials, nanoparticles, and biological systems.

R. O. Jones obtained his B.Sc. Hons (Physics) at the University of Western Australia in Perth and his Ph.D. at the University of Cambridge, England under Volker Heine. He spent three years as a Post-doctoral Associate at Cornell University before joining the FZ Jülich. His main interests for over 30 years have been density functional theory and its application to a wide range of systems (atoms, clusters, molecules, surfaces, ordered and disordered systems, ..).